Biosystems Diversity

ISSN 2519-8513 (Print)
ISSN 2520-2529 (Online)
Biosyst. Divers.

Molecular evidence for the taxonomic resurrection of *Stenurella sennii* nom. res. within the phylogeographic framework of *S. melanura* (Coleoptera, Cerambycidae)

S. Melnyk*, V. Malaniy*, Y.-Y. Kasicki*, O. Piddubnyi*, O. Pozniak*, L. Felbaba-Klushyna**, V. Shparyk*, O. Zinenko***, A. Zamoroka*

** Vasyl Stefanyk Carpathian National University, Ivano-Frankivsk, Ukraine*
*** Uzhhorod National University, Uzghorod, Ukraine*
**** V. N. Karazin Kharkiv National University, Kharkiv, Ukraine*

Article info
Received 05.01.2026
Received in revised form 03.02.2026
Accepted 18.02.2026

Vasyl Stefanyk Carpathian National University, Shevchenko St., 56, Ivano-Frankivsk, 76018, Ukraine. Tel.: +38-050-250-97-09. E-mail: andrii.zamoroka@cnu.edu.ua

Uzhhorod National University, Voloshyn St., 32, Uzghorod, 88000, Ukraine. Tel.: +38-099-054-08-89. E-mail: lyubov.felbaba-klushyna @uzhnu.edu.ua

V. N. Karazin Kharkiv National University, Svobody Sq., 4, Kharkiv, 61022, Ukraine. Tel.: +38-066-191-08-67. E-mail: oleksandrzinenko@karazin.ua

Melnyk, S., Malaniy, V., Kasicki, Y.-Y., Piddubnyi, O., Pozniak, O., Felbaba-Klushyna, L., Shparyk, V., Zinenko, O., & Zamoroka, A. (2026). Molecular evidence for the taxonomic resurrection of Stenurella sennii nom. res. within the phylogeographic framework of S. melanura (Coleoptera, Cerambycidae). Biosystems Diversity, 34(1), e2602. doi:10.15421/012602

We utilized DNA barcoding to analyze 241 mitochondrial COI sequences of *Stenurella melanura* across its European range, establishing a framework for understanding its intraspecific genetic variation with four genetically distinct haplogroups (*Sm1*–*Sm4*). The two most widespread lineages, *Sm1* and *Sm2*, show a strong association with dorsal pubescence coloration, particularly of the elytra: *Sm1* is dominated by light-pubescent individuals, whereas *Sm2* predominantly comprises dark-pubescent forms. Instances of discordance between haplogroup and pubescence coloration are best explained by ongoing hybridization, with geographically structured distributions across Europe, reflecting complex postglacial biogeography. Phylogenetic analysis revealed two highly divergent sequences forming a distinct clade, separated from *S. melanura* by a mean genetic distance of 0.077 substitutions per site. Morphological examination confirmed their conformity with the original description of *Stenurella sennii* **nom. res.**, validating the taxonomic restoration of this neglected species. As *S. sennii* **nom. res.** is a cryptic sibling species morphologically indistinguishable from light-pubescent *Sm1* haplogroup of *S. melanura*, traditional identification fails to capture this diversity. Our pan-European phylogeographic framework resolves this confusion, demonstrating that molecular diagnostics are essential for accurate species delimitation and for maintaining the integrity of taxonomic inventories.

Keywords: biodiversity; saproxylic beetles; cryptic species; DNA barcoding; COI; phenotypic polymorphism; hybridization; speciation; genetic divergence; integrative taxonomy.

Introduction

The genus *Stenurella* Villiers, 1974 (Coleoptera: Cerambycidae: Lepturinae) comprises a small group of Palaearctic longhorn beetles traditionally characterized by slender bodies, shortened elytra, and pronounced sexual dimorphism in coloration and body proportions (Villiers, 1974; Sama, 2002). Although these traits have long been used for diagnosis, they obscure substantial underlying evolutionary divergence within the group (Semaniuk & Zamoroka, 2020; Zamoroka et al., 2022). Consequently, the taxonomy and phylogeny of *Stenurella* have undergone major revision as research has shifted from purely morphological descriptions toward integrative systematic approaches (Crowley et al., 2024).

Phylogenetic analyses based on mitochondrial (16S rRNA, COI) and nuclear (28S rRNA) markers have demonstrated that *Stenurella* is polyphyletic, leading to the transfer of several species such as *S. nigra* (Linnaeus, 1758), *S. septempunctata* (Fabricius, 1793), and *S. vaucheri* (Bedel, 1900) to the genus *Rutpela* Thomson, 1864 (Zamoroka et al., 2022). These taxa belong to two deeply divergent evolutionary lineages within Lepturinae. *Stenurella* sensu stricto (e.g., *S. jaegeri* [Hummel, 1825], *S. novercalis* [Reitter, 1901], *S. bifasciata* [O. F. Müller, 1776], *S. melanura* [Linnaeus, 1758], *S. hybridula* [Reitter, 1902], and *S. approximans* [Rosenhauer, 1856]) is closely related to *Judolia* Mulsant, 1863 and *Anoplodera* Mulsant, 1839. By contrast, *Rutpela* (e.g., *R. nigra* **stat. res.**, *R. maculata* [Poda, 1761], *R. inermis* [K. Daniel & J. Daniel, 1898], *R. vaucheri* **stat. res.**, and *R. septempunctata* **stat. res.**) is phylogenetically allied with *Leptura* Linnaeus, 1758, *Stictoleptura* Casey, 1924, and related genera (Semaniuk & Zamoroka, 2020; Zamoroka et al., 2022).

Stenurella melanura represents one of the most common and widely distributed lepturine species in the Palaearctic, occurring from Western Europe through Siberia and extending into parts of West and East Siberia (Löbl & Smetana, 2010). It is also one of the most taxonomically problematic species within the tribe Lepturini, exhibiting extreme morphological plasticity across its range. Most variation involves subtle differences in pubescence, integument sculpture, and coloration patterns (Sama, 2002; Rapuzzi & Sama, 2009; Danilevsky, 2014; Vitali, 2018). The taxonomic stability of the *S. melanura* has long been challenged by pronounced chromatic polymorphism, leading to repeated attempts to delimit taxa based primarily on external coloration. This has gradually necessitated a shift toward analyses emphasizing structural morphology and DNA barcoding rather than pattern-based identification (Zamoroka et al., 2022).

Currently, the intraspecific taxonomy of *S. melanura* remains largely artificial and reflects historical taxonomic conventions rather than clearly delimited evolutionary units. Several taxa within this complex such as *S. samai* Rapuzzi, 1995, *S. sennii* Sama, 2002, *S. pamphyliae* Rapuzzi & Sama, 2009, and *S. zehrae* Özdikmen, Mercan & Cihan, 2012 have been variously treated as valid species, subspecies, or junior synonyms of *S. melanura* (Löbl & Smetana, 2010; Danilevsky, 2014; Vitali, 2018; Zamoroka et al., 2022). Subsequent taxonomic revisions incorporating broader morphological comparisons and nomenclatural assessments have generally synonymized these names under *S. melanura*, interpreting them as subspecific or phenotypic variations rather than distinct species. For example, *S. sennii* has been synonymized as a phenotypic variation of *S. melanura*, whereas *S. samai*, *S. zehrae*, and *S. pamphyliae* have been regarded as infraspecific entities within *S. melanura* (Danilevsky, 2014; Vitali, 2018).

While the historical descriptions relied heavily on variable elytral melanism, some recent revisions have retained subspecific taxa such as *S. melanura samai*, *S. melanura pamphyliae*, and *S. melanura zehrae* based on diagnostic morphological characters, particularly prono-

tal microsculpture, elytral punctation density, pubescence, and elytral coloration (Özdikmen et al., 2012). By contrast, the validity of *S. sennii* has generally been rejected due to overlapping diagnostic characters and syntopy with *S. melanura* throughout Europe (Danilevsky, 2014; Vitali, 2018). As a result, most morphology-based catalogues currently subsume all these names under *S. melanura*, reflecting a prevailing consensus that the observed morphological variation does not justify species-level recognition in the absence of discrete and consistent character sets. This case exemplifies the broader challenges of morphology-based taxonomy in widely distributed and phenotypically plastic taxa.

Despite its wide trans-Palaearctic distribution, the phylogeographic structure of *S. melanura* remains largely unexplored, with most available molecular data generated in the context of genus-level systematics rather than population-level analyses (Semaniuk & Zamoroka, 2020; Zamoroka et al., 2022). While recent phylogenetic studies employing mitochondrial (16S rRNA, COI) and nuclear (28S rRNA) markers have successfully demonstrated the polyphyly of *Stenurella* and justified the reclassification of several species into *Rutpela* (Zamoroka et al., 2022), they did not address genetic divergence within the *S. melanura* complex itself. Although public repositories such as BOLD and GenBank contain numerous COI barcode sequences attributed to *S. melanura*, no comprehensive phylogeographic analyses have been conducted to evaluate haplotype structure or to test the taxonomic validity of disputed taxa such as *S. sennii*, *S. pamphyliae*, *S. samai*, or *S. zehrae*. The recent publication of the complete mitochondrial and nuclear genomes of *S. melanura* (Crowley et al., 2024) provides an important genomic reference, but it represents a single haplotype from the United Kingdom and thus offers limited insight into genetic variation across the species' range. Consequently, key questions concerning historical population connectivity, glacial refugia, and postglacial expansion remain unresolved. By contrast, phylogeographic studies of other lepturine taxa have revealed pronounced haplogroup structuring correlated with geography (Zamoroka et al., 2019, 2024; Çakmak et al., 2020; Zamoroka & Zinenko, 2025), highlighting the potential of molecular approaches for resolving the *S. melanura* complex.

In the present study, we provide the most comprehensive molecular phylogeographic analysis of the *Stenurella melanura* to date, utilizing a robust dataset of cytochrome *c* oxidase subunit I (COI) sequences from across the West Palearctic. Significantly, this dataset includes newly generated sequences from Ukraine, marking the first molecular characterization of the species from this region. Our analysis reveals a deep genetic structure characterized by several distinct haplogroups, indicating a history of long-term isolation within glacial refugia rather than a single panmictic population. Crucially, we recovered a divergent molecular lineage that exhibits strict congruence with the morphological diagnostic characters historically attributed to *Stenurella sennii* **nom. res.**, distinct from the nominative *S. melanura* clade. These combined molecular and morphological findings provide compelling evidence for the specific status of this taxon, supporting the official reinstatement of *S. sennii* from synonymy.

Materials and methods

Sample collections. Fieldwork was conducted in 2020 at the National Park Syniohora in the Eastern Carpathians, Ukraine. During these surveys, adult specimens of *S. melanura* were collected and immediately preserved in 96% ethanol to prevent DNA degradation. All samples were individually labeled and transported to the laboratory, where they were stored at –20 °C. Voucher specimens are deposited in the collection of Vasyl Stefanyk Carpathian National University (PUIF).

DNA extraction. Extraction of DNA was performed from hind leg muscle tissue using a direct lysis protocol adapted from Korlević et al. (2021). Tissue samples were placed in individual wells of a 96-well plate, to which 25 µL of lysis buffer C (200 mM Tris pH 8.0, 25 mM EDTA pH 8.0, 0.05% Tween-20, and 0.4 mg/mL Proteinase K) was added. To ensure uniform buffer distribution and facilitate complete cell lysis, the tissue was homogenized and incubated at 56 °C for 2 hours. Following incubation, the lysate was diluted 10-fold; subsequent PCR reactions were performed directly on this unpurified DNA solution to optimize processing efficiency (Korlević et al. 2021; Makunin et al. 2022).

PCR. Amplification of the COI barcode region was performed using the indexed universal primers HCO and LCO (Srivathsan et al. 2021). Each 10 µL reaction mixture contained 5 µL of Master Mix, 0.3 µL each of forward and reverse primers, 0.7 µL of DNA template, 0.5 µL of dimethyl sulfoxide (DMSO), and 3.2 µL of distilled water. Components were mixed gently in thin-walled PCR tubes to minimize bubble formation. The thermal cycling profile consisted of an initial denaturation at 95 °C for 2 min, followed by 25–35 cycles of denaturation (95 °C for 30 s), annealing (40 °C for 30 s), and extension (72 °C for 45 s), concluding with a final extension at 72 °C for 5 min. Amplification success was verified by gel electrophoresis using a 2 µL aliquot of the PCR product, with the remainder stored at 4 °C for sequencing.

Library preparation and sequencing. Sequencing was conducted using the Oxford Nanopore Technologies (ONT) DNA-barcoding workflow outlined by Srivathsan et al. (2021). The products of PCR, containing unique index combinations, were pooled and purified prior to library preparation according to standard ONT protocols. Sequencing was performed on a MinION flow cell. Base calling was executed using ONT's proprietary software, while demultiplexing and consensus sequence generation were carried out using the ONTbarcoder 2.0 pipeline (Srivathsan et al. 2024).

Phylogenetic analysis. Phylogenetic reconstruction was conducted in Seaview 5.0 (Gouy et al., 2021). Sequence alignments were generated using the integrated MUSCLE algorithm, followed by manual inspection to excise ambiguous or poorly aligned regions. Maximum-likelihood (ML) trees were inferred via the PhyML module (Guindon et al., 2010) employing the General Time-Reversible (GTR) substitution model. Topology optimization utilized a combination of Nearest-Neighbor Interchange (NNI) and Subtree Pruning and Regrafting (SPR), with branch lengths refined via the BioNJ algorithm (Gascuel, 1997). Branch support was assessed using the Approximate Likelihood-Ratio Test (aLRT) (Anisimova & Gascuel, 2006; Guindon et al., 2010). The final phylogenetic dataset comprised 250 DNA barcode sequences (Table 1), including 241 specimens of *S. melanura*, 2 specimens of *S. sennii*, and 7 specimens of the outgroup (5 specimens of *S. bifasciata* and 2 specimens of *Anastrangalia dubia*).

Geographic range mapping. Distribution maps were generated using DIVA-GIS software (version 7.5.0.0). An occurrence matrix comprising 241 records of *S. melanura* was compiled in UTF-8 format, with coordinates standardized to the WGS 84 projection (EPSG: 4326) prior to import.

Table 1
DNA barcode vouchers, used in this study, including *Stenurella melanura*, and *Stenurella sennii* **nom. res.**, and outgroup

ID	Voucher number	Geographical coordinates
	Ingroup	
	Stenurella melanura	
1	GBCOU9046-15 (BS)	47.855, 11.487
2	GMGMA569-14 (BS)	50.5557, 7.16988
3	GMGMK1074-14 (BS)	50.5557, 7.16988
4	GMGMK1076-14 (BS)	50.5557, 7.16988
5	GMGMK787-14 (BS)	50.5557, 7.16988
6	GMGMK796-14 (BS)	50.5557, 7.16988
7	GMGML1202-14 (BS)	50.5557, 7.16988
8	CBGPC1005-21 (BS)	43.696037, 3.043569
9	CBGPC1006-21 (BS)	43.696037, 3.043569
10	CBGPC1007-21 (BS)	43.696037, 3.043569
11	CBGPC1008-21 (BS)	43.696037, 3.043569
12	CBGPC1009-21 (BS)	43.696037, 3.043569
13	CBGPC1010-21 (BS)	43.696037, 3.043569
14	CBGPC1019-21 (BS)	43.696037, 3.043569
15	CBGPC1020-21 (BS)	43.696037, 3.043569
16	CBGPC1022-21 (BS)	43.696037, 3.043569
17	CBGPC1023-21 (BS)	43.696037, 3.043569
18	CBGPC2033-21 (BS)	46.981647, 0.439079

ID	Voucher number	Geographical coordinates
19	CBGPC2044-21 (BS)	43.293667, 6.287893
20	CBGPC2309-21 (BS)	47.18424, 1.00448
21	CBGPC515-21 (BS)	43.653503, 6.733266
22	CBGPC635-21 (BS)	46.142227, 5.887869
23	CBGPC638-21 (BS)	46.142227, 5.887869
24	CBGPC639-21 (BS)	46.142227, 5.887869
25	CBGPC640-21 (BS)	46.117317, 5.939431
26	CBGPC642-21 (BS)	46.117317, 5.939431
27	CBGPC643-21 (BS)	46.117317, 5.939431
28	CBGPC644-21 (BS)	46.117317, 5.939431
29	CBGPC667-21 (BS)	46.015907, 5.964513
30	CBGPC687-21 (BS)	43.668324, 6.232389
31	CBGPC731-21 (BS)	46.36765, 6.018364
32	CBGPC749-21 (BS)	46.058563, 5.915414
33	CBGPC750-21 (BS)	46.058563, 5.915414
34	CBGPC784-21 (BS)	46.084396, 5.916551
35	CBGPC823-21 (BS)	46.142227, 5.887869
36	CBGPC844-21 (BS)	46.356087, 6.774322
37	CBGPC845-21 (BS)	46.356087, 6.774322
38	CBGPC995-21 (BS)	43.696037, 3.043569
39	CBGPC996-21 (BS)	43.696037, 3.043569
40	CBGPC999-21 (BS)	43.696037, 3.043569
41	CLPFR050-21 (BS)	43.07, -0.505
42	CLPFR115-21 (BS)	42.90874, -0.419220
43	CLPFR117-21 (BS)	42.90874, -0.419220
44	COLFA529-12 (BS)	64.417, 27.677
45	DTNHM7901-23 (BS)	51.437035, -0.231737
46	EUCAR164-10 (BS)	51.6333, 7.4
47	FBCOC353-10 (BS)	48.303, 10.9539
48	FBCOE769-12 (BS)	50.835915, 12.983298
49	FBCOF425-12 (BS)	49.095158, 13.247317
50	GBCOU6066-14 (BS)	52.489, 13.262
51	GBCOU9047-15 (BS)	47.855, 11.487
52	GBMIX717-14 (BS)	50.58, 13
53	GCOL10143-16 (BS)	52.2113, 12.8713
54	GMGMK1073-14 (BS)	50.5557, 7.16988
55	GMGMK1080-14 (BS)	50.5557, 7.16988
56	GMGMK328-14 (BS)	50.5557, 7.16988
57	GMGMK789-14 (BS)	50.5557, 7.16988
58	GMGMK792-14 (BS)	50.5557, 7.16988
59	GMGMK800-14 (BS)	50.5557, 7.16988
60	GMGRE2814-13 (BS)	48.9509, 13.4225
61	GMGRE2818-13 (BS)	48.9509, 13.4225
62	GMGRG4880-13 (BS)	48.9509, 13.4225
63	GRAEL1387-22 (BS)	47.8285, 1.913813
64	PLPOL818-23 (BS)	60.048, 19.984
65	POMS5132-24 (BS)	51.51053, -1.0430588
66	POMS5215-24 (BS)	51.509247, -1.040261
67	POMS5268-24 (BS)	51.51077, -1.0458132
68	POMS5271-24 (BS)	51.51077, -1.0458132
69	POMS5274-24 (BS)	51.51077, -1.0458132
70	PSFOR1136-17 (BS)	48.757973, 6.494574
71	PSFOR162-13 (BS)	47.830748, 1.925636
72	PSFOR453-13 (BS)	48.763, 2.242
73	PSFOR987-14 (BS)	49.006, 2.013
74	TDAAT1097-20 (BS)	48.171, 16.071
75	TDAAT1206-20 (BS)	47.536, 11.92
76	TDAAT552-19 (BS)	47.0167, 12.7758
77	CBGPC1018-21 (BS)	43.696037, 3.043569
78	CBGPC637-21 (BS)	46.142227, 5.887869
79	CBGPC730-21 (BS)	46.36765, 6.018364
80	CBGPC793-21 (BS)	43.331005, 5.75481
81	GMGMK788-14 (BS)	50.5557, 7.16988
82	NOCLP2021-20 (BS)	59.971, 10.731
83	CBGPC1004-21 (BS)	43.696037, 3.043569
84	CBGPC1021-21 (BS)	43.696037, 3.043569
85	CBGPC1024-21 (BS)	43.696037, 3.043569
86	CBGPC1096-21 (BS)	43.620792, 6.802085
87	CBGPC1097-21 (BS)	43.620792, 6.802085
88	CBGPC1140-21 (BS)	43.677994, 6.681774
89	CBGPC1141-21 (BS)	43.677994, 6.681774
90	CBGPC1145-21 (BS)	43.617653, 6.807396
91	CBGPC1146-21 (BS)	43.617653, 6.807396
92	CBGPC1158-21 (BS)	43.33741, 5.773746
93	CBGPC1159-21 (BS)	43.33741, 5.773746
94	CBGPC1181-21 (BS)	43.33741, 5.773746
95	CBGPC1182-21 (BS)	43.33741, 5.773746
96	CBGPC1183-21 (BS)	43.33741, 5.773746
97	CBGPC1184-21 (BS)	43.33741, 5.773746
98	CBGPC1185-21 (BS)	43.33741, 5.773746
99	CBGPC1186-21 (BS)	43.33741, 5.773746
100	CBGPC1187-21 (BS)	43.33741, 5.773746
101	CBGPC1188-21 (BS)	43.33741, 5.773746
102	CBGPC1199-21 (BS)	43.620792, 6.802085
103	CBGPC1200-21 (BS)	43.620792, 6.802085
104	CBGPC1513-21 (BS)	43.745483, 6.82775
105	CBGPC1514-21 (BS)	43.745483, 6.82775
106	CBGPC1562-21 (BS)	44.011627, 7.254947
107	CBGPC1581-21 (BS)	43.98715, 6.624019
108	CBGPC1582-21 (BS)	43.98715, 6.624019
109	CBGPC1583-21 (BS)	43.98715, 6.624019
110	CBGPC1870-21 (BS)	43.788204, 6.689176
111	CBGPC1907-21 (BS)	43.95222, 7.347942
112	CBGPC1934-21 (BS)	44.00449, 7.471411
113	CBGPC1939-21 (BS)	43.984016, 7.40285
114	CBGPC1944-21 (BS)	43.9763, 7.412225
115	CBGPC1949-21 (BS)	43.99707, 7.506371
116	CBGPC1955-21 (BS)	43.984016, 7.40285
117	CBGPC2032-21 (BS)	46.981647, 0.439079
118	CBGPC2051-21 (BS)	43.293667, 6.287893
119	CBGPC2052-21 (BS)	43.293667, 6.287893
120	CBGPC2053-21 (BS)	43.293667, 6.287893
121	CBGPC2069-21 (BS)	43.293667, 6.287893
122	CBGPC2070-21 (BS)	43.293667, 6.287893
123	CBGPC2158-21 (BS)	44.317936, 6.6315
124	CBGPC2165-21 (BS)	44.206936, 6.742633
125	CBGPC2295-21 (BS)	47.2379, 0.965574
126	CBGPC580-21 (BS)	44.04088, 7.243874
127	CBGPC601-21 (BS)	46.36765, 6.018364
128	CBGPC603-21 (BS)	46.23624, 5.820295
129	CBGPC633-21 (BS)	46.142227, 5.887869
130	CBGPC634-21 (BS)	46.142227, 5.887869
131	CBGPC636-21 (BS)	46.142227, 5.887869
132	CBGPC641-21 (BS)	46.117317, 5.939431
133	CBGPC645-21 (BS)	46.117317, 5.939431
134	CBGPC666-21 (BS)	46.015907, 5.964513
135	CBGPC668-21 (BS)	46.015907, 5.964513
136	CBGPC729-21 (BS)	46.36765, 6.018364
137	CBGPC751-21 (BS)	46.015907, 5.964513
138	CBGPC752-21 (BS)	46.015907, 5.964513
139	CBGPC785-21 (BS)	46.084396, 5.916551
140	CBGPC794-21 (BS)	43.331005, 5.75481
141	CBGPC795-21 (BS)	43.331005, 5.75481
142	CBGPC821-21 (BS)	46.142227, 5.887869
143	CBGPC822-21 (BS)	46.142227, 5.887869
144	CBGPC824-21 (BS)	44.0658, 3.570409
145	CBGPC825-21 (BS)	44.0658, 3.570409
146	CBGPC880-21 (BS)	43.78326, 6.600032
147	CBGPC881-21 (BS)	43.78326, 6.600032
148	CBGPC896-21 (BS)	43.750343, 6.647127
149	CBGPC897-21 (BS)	43.750343, 6.647127
150	CBGPC898-21 (BS)	43.750343, 6.647127
151	CBGPC899-21 (BS)	43.750343, 6.647127
152	CBGPC900-21 (BS)	43.750343, 6.647127
153	CBGPC901-21 (BS)	43.750343, 6.647127
154	CBGPC902-21 (BS)	43.750343, 6.647127
155	CBGPC927-21 (BS)	46.015907, 5.964513
156	CBGPC928-21 (BS)	46.015907, 5.964513
157	CBGPC997-21 (BS)	43.696037, 3.043569
158	CBGPC998-21 (BS)	43.696037, 3.043569
159	CLPFR018-21 (BS)	42.80979, 0.55732
160	CLPFR019-21 (BS)	42.80979, 0.55732
161	CLPFR025-21 (BS)	44.08722, 7.30367
162	CLPFR026-21 (BS)	42.51012, 2.22319
163	CLPFR027-21 (BS)	42.51012, 2.22319
164	CLPFR049-21 (BS)	43.07, -0.505
165	CLPFR051-21 (BS)	43.07, -0.505
166	CLPFR116-21 (BS)	42.90874, -0.419220
167	COLFA530-12 (BS)	64.417, 27.677
168	COLFA602-12 (BS)	61.565, 29.564
169	COLFE008-12 (BS)	61.528, 27.16
170	COLFE663-13 (BS)	60.514, 26.886
171	COLFE752-13 (BS)	60.314, 24.258
172	PV658013 (GB)	48.584737, 24.171553

ID	Voucher number	Geographical coordinates
173	COLHH2712-19 (BS)	59.4313, 9.05228
174	DTNHM5191-23 (BS)	51.188206, 0.117129
175	FBCOF1062-12 (BS)	50.00387, 7.804845
176	FBCOF390-12 (BS)	49.070045, 13.131831
177	FBCOF464-12 (BS)	49.02829, 13.308509
178	GBCLC1961-19 (BS)	–
179	GBCLC1964-19 (BS)	52.882794, 18.727671
180	GBCLC1965-19 (BS)	52.671745, 23.796728
181	GBCOC168-12 (BS)	50.59876, 13.1484
182	GBCOL545-12 (BS)	47.14685, 11.560465
183	GBCOL563-12 (BS)	47.013485, 11.306542
184	GBCOU4727-14 (BS)	52.276, 12.523
185	GBCOU5055-14 (BS)	52.445, 12.831
186	GBCOU5368-14 (BS)	52.444, 12.725
187	GBCOU5969-14 (BS)	48.303, 10.973
188	GBCOU9045-15 (BS)	47.855, 11.487
189	GCOL10144-16 (BS)	52.2113, 12.8713
190	GCOL1144-16 (BS)	51.3031, 11.1359
191	GCOL11767-16 (BS)	51.7111, 10.7409
192	GCOL12246-16 (BS)	53.4048, 12.866
193	GCOL3966-16 (BS)	45.8611, 7.55138
194	GMGMJ903-14 (BS)	50.5557, 7.16988
195	GMGMK1075-14 (BS)	50.5557, 7.16988
196	GMGMK329-14 (BS)	50.5557, 7.16988
197	GMGMK330-14 (BS)	50.552, 7.17
198	GMGMK331-14 (BS)	50.5557, 7.16988
199	GMGMK790-14 (BS)	50.5557, 7.16988
200	GMGMK805-14 (BS)	50.5557, 7.16988
201	GMGML1206-14 (BS)	50.5557, 7.16988
202	GMGML281-14 (BS)	50.5557, 7.16988
203	GMGML283-14 (BS)	50.5557, 7.16988
204	GRAEL1386-22 (BS)	47.8285, 1.913813
205	GRAEL2202-23 (BS)	47.277, 0.905
206	ICRYO015-22 (BS)	44.953, 15.528
207	NLCOD037-15 (BS)	51.131, 6.086
208	NOCLP2022-20 (BS)	60.514, 12.122
209	PLPOL819-23 (BS)	60.211, 20.09
210	PLPOL820-23 (BS)	60.046, 19.978
211	PLPOL821-23 (BS)	60.046, 19.978
212	PLPOL822-23 (BS)	60.046, 19.978
213	POMS1155-24 (BS)	51.507496, -1.038410
214	PSFOR452-13 (BS)	48.763, 2.242
215	PSFOR454-13 (BS)	48.763, 2.242
216	TDAAT1119-20 (BS)	48.219, 16.23
217	TDAAT945-20 (BS)	48.17, 16.096
218	TDAOE3018-23 (BS)	48.2208, 16.2731
219	GMGMK1077-14 (BS)	50.5557, 7.16988
220	TDAOE3219-23 (BS)	48.211666, 16.261667
221	FBCOJ409-12 (BS)	50.75, 4.423
222	GBCOL200-12 (BS)	51.177303, 12.482473
223	GBCOU5367-14 (BS)	52.444, 12.725
224	GBCOU6068-14 (BS)	52.489, 13.262
225	GCOL1041-16 (BS)	50.8622, 11.2975
226	GCOL1053-16 (BS)	50.8907, 11.172
227	GCOL12247-16 (BS)	53.4048, 12.866
228	GMGML1203-14 (BS)	50.5557, 7.16988
229	GMGML1468-14 (BS)	50.5557, 7.16988
230	GMGRF5273-13 (BS)	48.9509, 13.4225
231	GMGRG4881-13 (BS)	48.9509, 13.4225
232	GRAEL1263-22 (BS)	42.772, -0.335
233	PHDLV266-22 (BS)	47.84987, 2.16473
234	GBCOU7053-14 (BS)	45.53, 6.172
235	OY757319.1 (GB)	52.756501, -2.017166
236	BSBPL251-25 (BS)	52.722973, 23.85363
237	BSBPL250-25 (BS)	49.69952, 22.541763
238	BSBPL249-25 (BS)	50.932877, 20.908945
239	BSBPL248-25 (BS)	50.948597, 17.331524
240	BSBPL247-25 (BS)	51.47857, 16.92432
241	BSBPL246-25 (BS)	51.516350, 15.759900
	Stenurella sennii nom. res.	
242	PSFOR160-13 (BS)	45.382, 2.4939
243	PSFOR1138-17 (BS)	47.812780, 0.4186109
	Outgroup	
	Stenurella bifasciata	
244	KU919187 (GB)	51.48, 13.82
245	KM450273 (GB)	50.5194, 7.04022
246	KM285769 (GB)	43.197, 6.329
247	KM447494 (GB)	50.5243, 7.03716
248	PV658012 (GB)	46.910315, 30.980384
	Anastrangalia dubia	
249	PV658002 (GB)	48.482836, 24.527862
250	PV657999 (GB)	48.130177, 24.613737

Notes: BS – BOLDSystems; GB – GenBank.

Results

Genetic diversity of S. melanura. We analyzed 241 sequences (Fig. 1) of *S. melanura* and found that within the European part of its range, four genetically distinct lineages are present. We identified these lineages as haplogroups *Sm1*, *Sm2*, *Sm3*, and *Sm4* (Fig. 2).

Haplogroup *Sm1* is represented by 148 analyzed sequences. This haplogroup comprises four well-defined clusters of sequences, which we delineated as separate haplotypes: *Sm1-h1*, *Sm1-h2*, *Sm1-h3*, and *Sm1-h4*. The mean genetic distance among sequences within haplogroup *Sm1* is 0.009 substitutions per site (Fig. 1). Intragroup genetic distances within haplotypes range from 0.001 to 0.006 substitutions per site, whereas intergroup distances range from 0.007 to 0.015 substitutions per site.

Haplogroup *Sm2* is represented by 34 analyzed sequences. This haplogroup includes six well-defined clusters of sequences, which were identified as separate haplotypes: *Sm2-h1*, *Sm2-h2*, *Sm2-h3*, *Sm2-h4*, *Sm2-h5*, and *Sm2-h6*. The mean genetic distance among sequences within haplogroup *Sm2* is 0.023 substitutions per site (Fig. 1). Intragroup genetic distances within haplotypes range from 0.000 to 0.006 substitutions per site, while intergroup distances range from 0.007 to 0.021 substitutions per site.

Haplogroup *Sm3* is represented by four analyzed sequences, which form a single compact cluster. The mean genetic distance among sequences within haplogroup *Sm3* is 0.023 substitutions per site (Fig. 1). Intragroup genetic distances within haplotypes are 0.001 substitutions per site.

Haplogroup *Sm4* is represented by 53 analyzed sequences. This haplogroup comprises five well-defined clusters of sequences, which we delineated as separate haplotypes: *Sm4-h1*, *Sm4-h2*, *Sm4-h3*, *Sm4-h4*, and *Sm4-h5*. The mean genetic distance among sequences within haplogroup *Sm4* is 0.006 substitutions per site (Fig. 1). Intragroup genetic distances within haplotypes range from 0.000 to 0.005 substitutions per site, whereas intergroup distances range from 0.002 to 0.011 substitutions per site.

An unexpected result of our study was the detection of a relationship between the identified COI haplogroups and external morphology. We analyzed available images of *S. melanura* in BOLD Systems and the sequences associated with them. We found that the two most widespread European haplogroups, *Sm1* and *Sm2* (Fig. 2), are associated with color variation of the dorsal body pubescence, primarily that of the elytra.

Specifically, among 148 sequenced specimens of *S. melanura* belonging to haplogroup *Sm1*, morphological information was available for 47 specimens (31.8%) (Fig. 1). Of these, 37 individuals (79%) exhibit a distinctly light yellow to golden pubescence, whereas 10 individuals (21%) are covered with dark brown to black setae. By contrast, within haplogroup *Sm2*, individuals with dark pubescence predominate, accounting for 55%, compared with 45% light-colored individuals. Notably, in some haplotypes, for example *Sm2-h2*, the proportion of dark forms reaches 90%. We also observed a tendency for dark-pubescent individuals to occur at higher latitudes and in mountainous regions of Europe (Fig. 3), whereas light morphs are more typical of lowland areas and southern Europe (Fig. 3).

Although all four identified haplogroups overlap completely or partially in their distributions, haplogroups *Sm3* and *Sm4* show restricted ranges in Western and Southwestern Europe (Fig. 3). By contrast, only two haplogroups, *Sm1* and *Sm2*, cover most of Europe (Fig. 3). As noted above, *Sm1* populations are characterized by a predominance of light-pubescent individuals, whereas *Sm2* populations are dominated by dark-pubescent individuals. It should be emphasized that COI is part of the non-recombining, maternally inherit-

ed mitochondrial genome, which has no direct phenotypic expression in morphology. Meanwhile, setal coloration is determined by the presence of melanin, which is encoded in the nuclear genome.

Essentially, our results indicate a long-term divergence of *S. melanura* populations representing each haplogroup, which correlates well with phenotypic differentiation and highlights linked inheritance of both mitochondrial and nuclear genomes. Such linkage provides evidence that each ancestral population passed through an evolutionary bottleneck in its history, resulting in the fixation of the observed phenotypes and COI haplogroups. However, the cases of haplogroup-phenotype discrepancy that we detected (Fig. 2)—namely *Sm1* combined with a dark-pubescent phenotype and *Sm2* combined with a light-pubescent phenotype—with a high degree of probability indicate hybridization between these lineages.

Specifically, within haplogroup *Sm1*, which generally corresponds to light-pubescent morphs, we detected dark-colored individuals, e.g. COLFA529-124; PLPOL818-23; PLPOL821-23; PLPOL822-23; POMS1155-24; PLPOL819-23; PLPOL820-23; NLCOD037-15; CLPFR018-21; and CLPFR116-21. Conversely, within haplogroup *Sm2*, individuals with light pubescence were identified, including GBCOL545-12; ICRYO015-22; CLPFR019-21; GBCOC168-12; GBCOU5055-14; TDAOE3219-23; GBCOU5367-14; GBCOU6068-14; FBCOJ409-12; and GBCOU7053-14. Dark-pubescent individuals carrying haplogroup *Sm1* typically occur in the Baltic region, Eastern Europe, and mountainous areas of Europe, whereas light-pubescent individuals carrying haplogroup *Sm2* are most frequently found in Southern Europe and in lowland regions of Western and Central Europe.

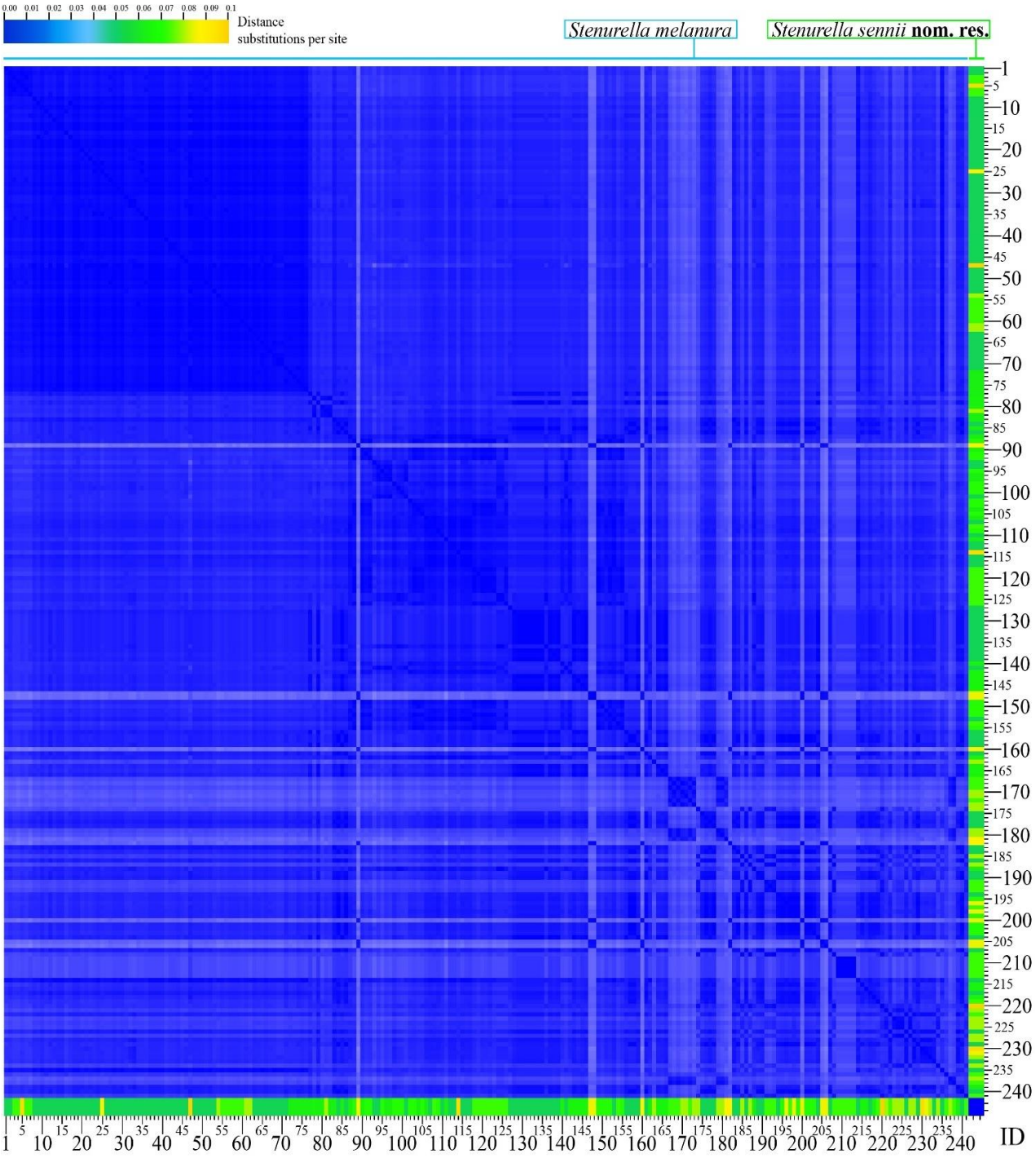

Fig. 1. Estimates of evolutionary divergence between sequences of *Stenurella melanura* and *Stenurella sennii* **nom. res.:** number of base substitutions per site between sequences is shown; for ID number see Table 1

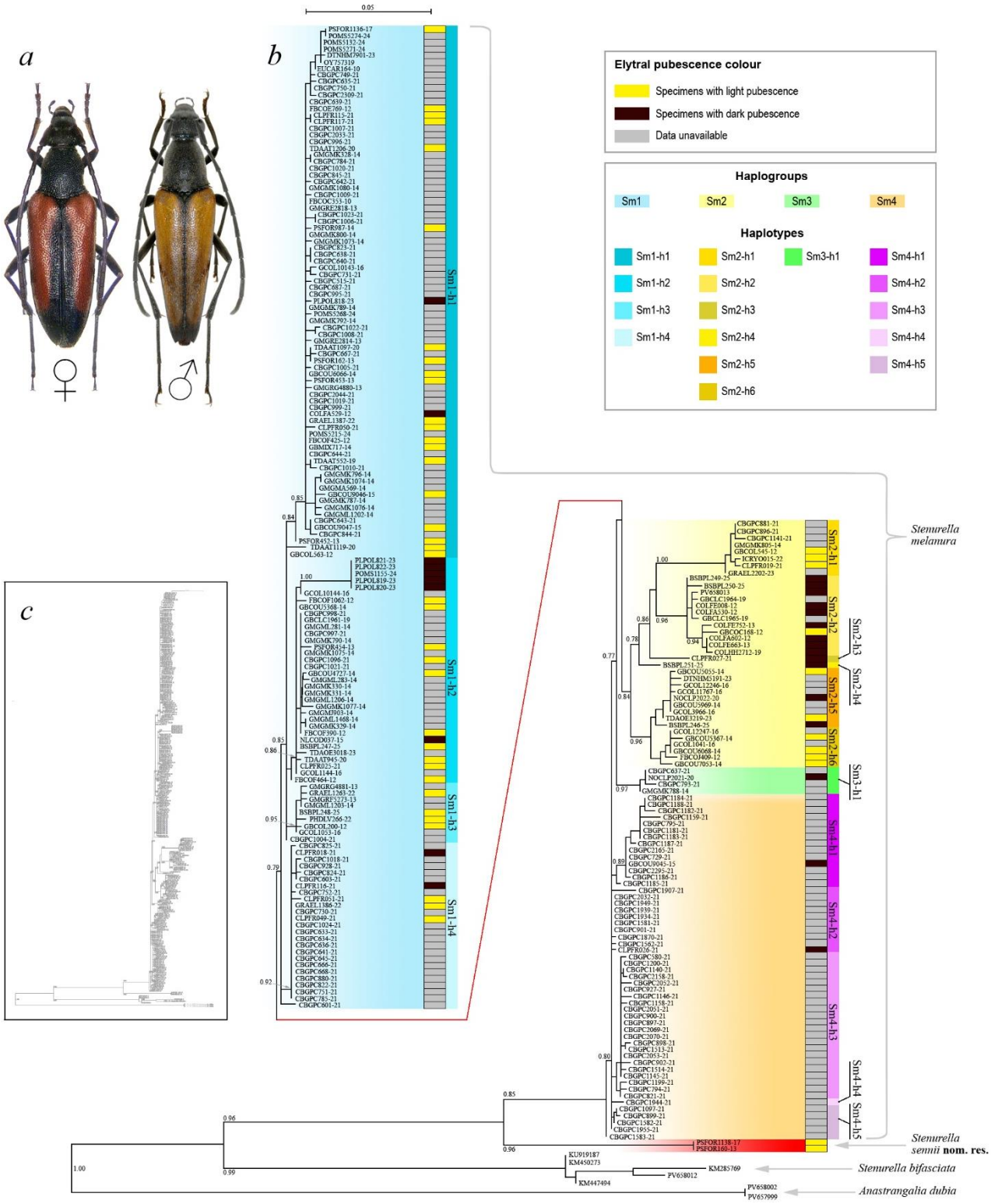

Fig. 2. Inter- and intraspecies phylogeny of *Stenurella melanura* revealed its complex haplogroup composition and distinction of *S. sennii* **nom. res**.

Together, these two markers, the genetic COI marker and the phenotypic color trait, form west-east and north-south distributional gradients, clearly illustrating postglacial secondary contact and hybridization-driven admixture of populations that likely originated in different glacial, and possibly preglacial, refugia.

Distinction of S. sennii ***nom. res.*** Within all 243 analyzed COI sequences preliminarily identified as *S. melanura*, we detected two sequences, PSFOR1138-17 and PSFOR160-13, that are markedly divergent from the remaining material and represented separate species – *S. sennii* **nom. res.** In the phylogenetic tree (Fig. 2), these two sequences form a separate clade, clearly isolated from *S. melanura*. Analysis of genetic distances (Table 2) between *S. sennii* **nom. res.** and *S. melanura* COI sequences yielded a value of 0.077 substitutions per site. The minimum divergence was 0.062 substitutions per site, whereas the maximum divergence reached 0.186 substitutions per site. For comparison, the mean intraspecific genetic distance within *S. melanura* sequences is 0.015 substitutions per site, with a minimum of 0.000 and a maximum of 0.05018 substitutions per site. By contrast, the mean genetic distance between *S. melanura* and *S. bifasciata*, two well-defined and deeply separated species belonging to different subgenera of *Stenurella*, amounts to 0.160 substitutions per site. According to the Student's t-test, the genetic divergence between the *S. melanura* main cluster and the resurrected *S. sennii* **nom. res.** lineage is highly statistically significant ($t = 72.93$, $P < 0.0001$).

Table 2
Pairwise matrix of mean COI genetic distances (substitutions per site; below diagonal) and Student's t-test results with P-values (above diagonal) for the studied species

Species	*Stenurella melanura*	*Stenurella sennii* **nom. res.**	*Stenurella bifasciata*	*Anastrangalia dubia*
S. melanura	0.015	$t = 72.93$ $P = 1.77\times10^{-202}$	$t = 327.59$ $P \approx 0.00$	$t = 426.99$ $P \approx 0.00$
S. sennii **nom. res.**	0.077	0.000	$t = 103.24$ $P = 6.00\times10^{-245}$	$t = 147.28$ $P = 9.22\times10^{-282}$
S. bifasciata	0.160	0.150	0.018	$t = 84.22$ $P = 4.01\times10^{-287}$
A. dubia	0.193	0.190	0.175	0.000

Morphological analysis of specimens PSFOR1138-17 and PSFOR160-13 (Fig. 4) demonstrated their complete conformity with the diagnostic criteria provided in the original description of *S. sennii* **nom. res.** (Sama, 2002), which provided sufficient grounds for a formal nomenclatural act restoring the validity of this species. At the same time, it must be emphasized that in terms of morphology, *S. sennii* **nom. res.** is very similar, and in some cases virtually identical, to the light-pubescent forms of *S. melanura* representing haplogroup *Sm1*.

Other than the COI genetic markers, we were unable to identify characters sufficient for reliable morphological discrimination between light-pubescent *S. melanura* and *S. sennii* **nom. res.** We also note the extreme rarity of *S. sennii* **nom. res.**, as among all 243 barcoded specimens, the species is represented by only two males (0.8%), both originating exclusively from France (Fig. 4).

Phylogeography of S. melanura. As shown above, at least four major haplogroups of *S. melanura* occur in Europe: *Sm1*, *Sm2*, *Sm3*, and *Sm4* (Fig. 2). Unfortunately, sequenced material is lacking from the major Mediterranean peninsulas and from Eastern Europe (east of the Carpathians), resulting in an incomplete phylogeographic picture of *S. melanura*. Nevertheless, the available data allow for certain extrapolations and enable reasonably realistic inferences regarding the species' genetic diversity, glacial refugia, and postglacial expansion.

Across most of Europe (from Fennoscandia to the Dinaric Alps) only two haplogroups, *Sm1* and *Sm2*, are present. These haplogroups widely overlap in Central and Western Europe (Fig. 3). Haplogroup *Sm1* is more widely distributed in Western and Central Europe, whereas *Sm2* predominates in Northern and Eastern Europe. Carriers of haplogroup *Sm1* occupy lowland and low-mountain regions across almost the entire known range of the species. In the south, however, this haplogroup occurs mainly in mountainous regions, such as the Pyrenees and the Maritime Alps. Meanwhle, haplogroup *Sm2* is widely distributed across the lowlands of Northern Europe, while in Central and Southern Europe it occurs almost exclusively in mountainous habitats characterized by cooler, boreal-like climatic conditions.

Haplogroups *Sm3* and *Sm4* are known only from Western and Southwestern Europe (Fig. 3). Available barcode data indicate a high frequency of haplogroup *Sm4* in Southern France, particularly in the region between the Pyrenees, the Alps, and the Massif Central. It is likely that carriers of this haplogroup also occur in mountainous areas of the Iberian and Apennine peninsulas. Haplogroup *Sm3*, despite its rarity, appears to occupy a very broad geographic range in Western Europe, extending from Southern Norway to Southern France. However, the overall distribution range of this haplogroup remains insufficiently resolved.

We demonstrate that three haplogroups (Sm1, Sm2, Sm4) possess a distinct phylogeographic structure indicative of glacial refugia and subsequent range expansion—processes central to historical biogeography. The primary refugium for haplogroup *Sm1* was likely Southern France, facilitating northward and eastward expansion during the Holocene. Current records of Sm1 within northern populations may represent relict biodiversity from the Atlantic time, the warmest period of Holocene, or evidence of more recent introgressive hybridization. Definitive classification of these lineages necessitates nuclear genetic analysis to disentangle these complex evolutionary pathways.

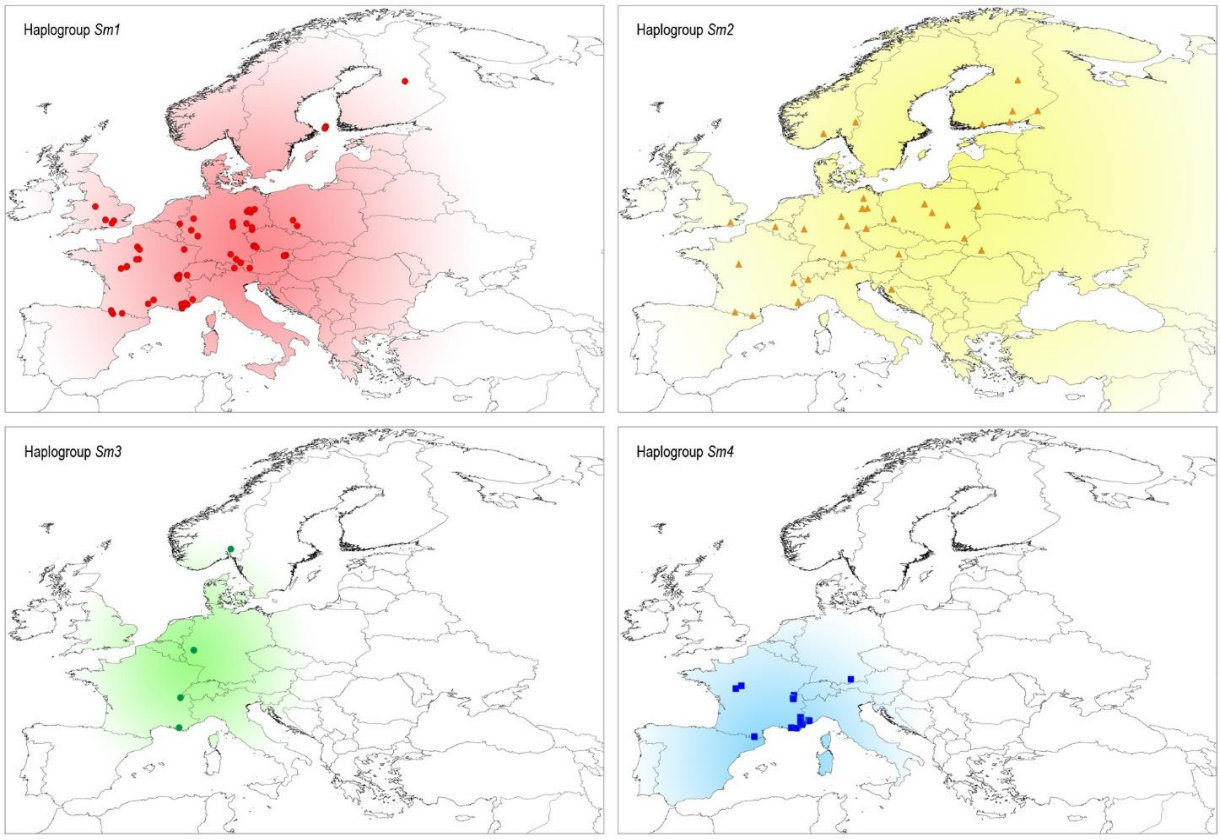

Fig. 3. Geographic patterns of *Stenurella melanura* haplogroups within Europe

The boreal distribution pattern of haplogroup *Sm2* in Europe, particularly in Fennoscandia, the Baltic region, and the mountains of Central Europe, suggests that its glacial refugium was located far to the east of the continent. Most likely, this refugium was situated in the Volga region or the Southern Urals, with postglacial expansion probably proceeding from east to west along a northern route, followed by penetration into the mountain systems of Europe. Future DNA barcoding of *S. melanura* from Eastern Europe and Siberia will be crucial for clarifying this hypothesis.

Carriers of haplogroup *Sm4* show a strong association with mountain ranges of the northwestern Mediterranean region, which directly indicates that their glacial refugium was located in this area. The most plausible natural candidate for the glacial refugium of *Sm4* is the Iberian Peninsula. Finally, the genetic markers of the two specimens of *S. sennii* **nom. res.** currently known from DNA barcoding have been detected only in central France, leaving the overall distribution range of this species entirely unknown. Numerous records from Central and Eastern Europe (see Discussion) are likely unrelated to this species.

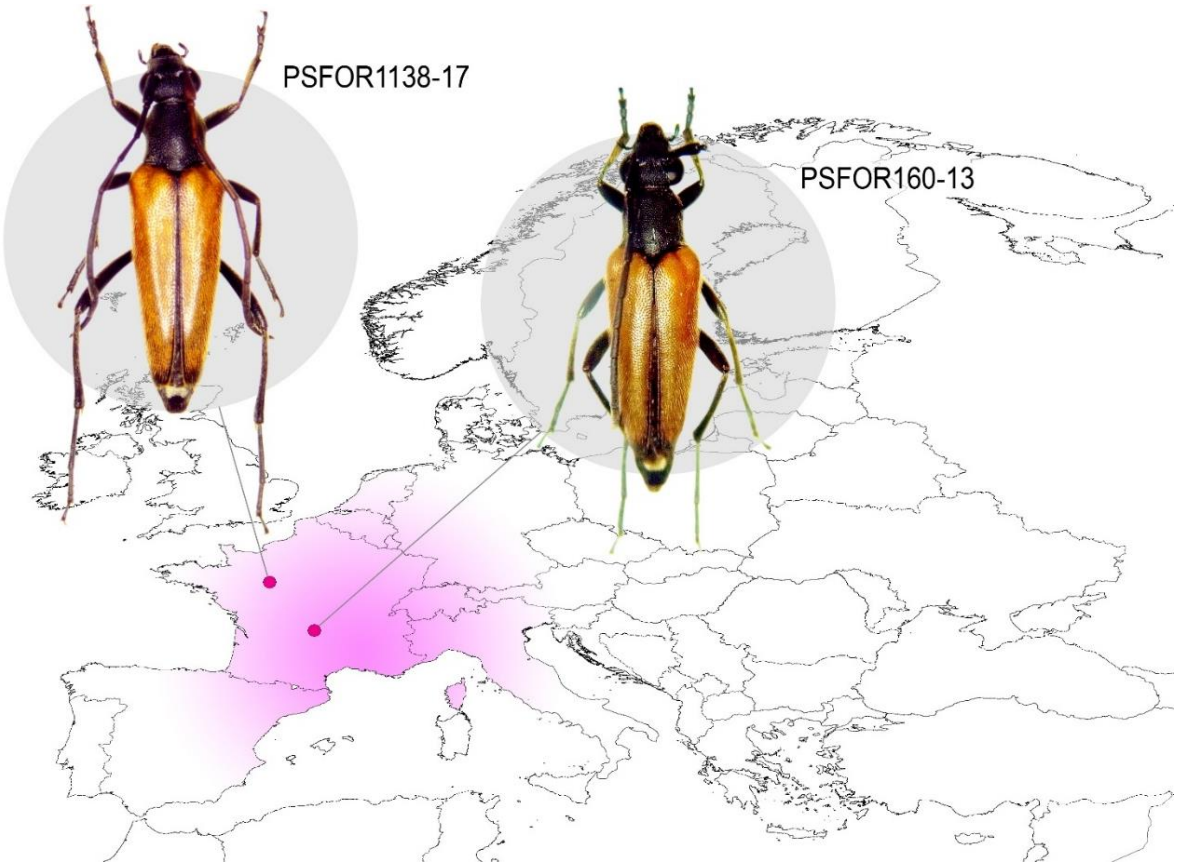

Fig. 4. European distribution of *Stenurella sennii* **nom. res.** based on COI DNA-barcoded records, with the habitus of confirmed specimens illustrated

Discussion

Stenurella melanura is the most widespread and abundant species of lepturine longhorn beetles in Europe (Danilevsky, 2014; Zamoroka et al., 2022). Nonetheless, its phylogeography remains extremely poorly studied. Zoogeographers classify the species as trans-Palaearctic, as it occurs across vast areas extending from the Atlantic coast in the west, throughout Europe and Siberia, to the Pacific coast in the east (Löbl & Smetana, 2010; Danilevsky, 2014). Across this range, the species exhibits numerous color-based morphological variants, which in the past led to their description as separate species, e.g. *S. samai*, *S. sennii* **nom. res.**, *S. pamphyliae*, and *S. zehrae* (Löbl & Smetana, 2010; Danilevsky, 2014; Vitali, 2018; Zamoroka et al., 2022). Over the last decade, a broad discussion has emerged regarding the validity of these taxa, and ultimately all of them were synonymized with *S. melanura*. In particular, *S. samai*, *S. pamphyliae*, and *S. zehrae* were proposed to be treated as geographical subspecies of *S. melanura* (Danilevsky, 2014), occurring mainly in the southeastern part of its range. By contrast, *S. sennii* **nom. res.** was downgraded to a junior synonym of *S. melanura* due to their morphological similarity and complete overlap of distribution ranges (Danilevsky, 2014; Vitali, 2018).

As noted by Vitali (2018), the morphological patterns proposed by Sama (2002) for identifying *S. sennii* **nom. res.** are widely distributed within *S. melanura* populations across Europe. In particular, Sama (2002) stated: "Males of *S. sennii* differ from those of *S. melanura* in having erect hairs on the head, the pronotum, the elytra and the pygidium golden yellow and thicker." The problem is that the key diagnostic character used by Sama (2002) was not the structure of the genitalia, but rather differences in pubescence coloration, which subsequently led to misinterpretation and the eventual synonymization of *S. sennii* **nom. res.**

In the present study, we demonstrate that light-pubescent individuals of *S. melanura* belong to a distinct genetic lineage, haplogroup *Sm1*, but do not exceed species-level boundaries and cannot be considered a subspecies. Moreover, we show that they freely hybridize with carriers of other COI haplogroups characterized by dark pubescence. We have previously demonstrated similar cases of hybridization in a number of other longhorn beetle species, occurring at both the subspecific level and below (Zamoroka et al., 2019; Zamoroka & Zinenko, 2025; Zamoroka, 2025).

Overall, due to the ambiguity of species criteria, a substantial confusion has arisen in the morphological discrimination between *S. melanura* carriers of haplogroup *Sm1* and *S. sennii* **nom. res.** This resulted in numerous records of *S. sennii* **nom. res.** from the Czech Republic (Rapuzzi et al., 2011), Croatia (Rapuzzi et al., 2011), Italy (Sama & Rapuzzi, 2011), and Ukraine (Zamoroka et al., 2012), followed later by the decision to synonymize both taxa (Danilevsky, 2014; Vitali, 2018) and exclusion from the national species lists (Zamoroka, 2022; Zamoroka, 2023).

In this study, we demonstrate that among sequenced individuals morphologically resembling *S. melanura*, there are specimens exhibi-

ting highly divergent genetic signatures. By integrating morphological traits with available genetic data (PSFOR1138-17 and PSFOR160-13), we conclude that these specimens actually belong to the recently-neglected species *S. sennii* **nom. res.**, which we propose to revalidate. It should be noted that an attempt to clarify the relationship between *S. sennii* **nom. res.** and *S. melanura* at the molecular level was made by Sire et al. (2019) within a broad DNA barcoding framework of saproxylic beetles in France. They found that *S. sennii* **nom. res.** differs from *S. melanura* by 7.11% (Sire et al., 2019: Table 3). However, they also noted that not all specimens identified morphologically as *S. sennii* **nom. res.** were genetically distinct from *S. melanura* (Sire et al., 2019: Table 4). Our results fully corroborate their findings, although they indicate a slightly higher mean divergence between *S. sennii* **nom. res.** and *S. melanura* (7.8%). We agree that the discrepancies between DNA barcodes and presumed species reported by Sire et al. (2019) are primarily due to errors in morphological identification of *S. sennii* **nom. res.**, which is in fact a challenging task even for experienced experts (Touroult et al., 2019). From this perspective, the pan-European phylogeographic analysis of *S. melanura* conducted here clearly separated barcoded specimens of *S. melanura* and *S. sennii* **nom. res.**, allowing them to be distinguished from light-pubescent forms of *S. melanura*.

We emphasize the rarity and restricted distribution range of *S. sennii* **nom. res.**, which constitutes only 0.8% of the total dataset and is currently confirmed only in France. This finding suggests that previous records from the Czech Republic, Croatia, Italy, and Ukraine (Rapuzzi et al., 2011; Sama & Rapuzzi, 2011; Zamoroka et al., 2012) are likely misidentified light-pubescent *S. melanura* (haplogroup Sm1) or hybrids with *Sm2*. Accurate delineation of these ranges is a prerequisite for correct biodiversity assessment and the evaluation of conservation status for these sibling species. Future morphological approaches to the identification of *S. sennii* **nom. res.** must therefore be revised, as the risk of misidentification is extremely high. At present, reliable identification of *S. sennii* **nom. res.** appears possible only through molecular analysis, as it is a cryptic sibling species of *S. melanura* that evolved relatively recently.

Future studies should encompass DNA barcoding across the entire range of *S. melanura* to elucidate both its genetic diversity and the true distribution of the cryptic species *S. sennii* **nom. res.** Another unresolved issue concerns the taxonomic status of the currently recognized subspecific taxa *S. melanura* samai, *S. melanura* pamphyliae, and *S. melanura* zehrae. Molecular methods may prove crucial in resolving this taxonomic conundrum. Broad-scale DNA barcoding will also facilitate the identification of glacial refugia, postglacial expansion routes, and the evolutionary history of *S. melanura*.

Conclusions

A continent-scale molecular phylogeographic framework allowed us to resolve a nearly quarter-century-long confusion surrounding the color forms of *S. melanura* and the long-forgotten species *S. sennii* **nom. res.** The application of molecular methods enabled us to characterize genetic diversity and its geographic patterns, identifying potential climate-driven glacial refugia and postglacial expansion routes. These findings validate and restore the taxonomic status of *S. sennii* **nom. res.**, providing critical baseline data for biodiversity assessment and species conservation efforts.

The study was conducted as part of the ongoing scientific research project titled "Molecular phylogeny and systematics of living organisms" (state registration number 0121U109305) at Vasyl Stefanyk Carpathian National University. O.Z. have also received support through the EURIZON project, which is funded by the European Union under grant agreement No.871072, and laboratory work was possible due to the support of the Academic Sanctuaries Fund created by XTX Markets. The sequences were obtained as a part of training activities of Biodiversity Genomics Europe (Grant no.101059492), funded by Horizon Europe under the Biodiversity, Circular Economy and Environment call (REA.B.3); cofunded by the Swiss State Secretariat for Education, Research and Innovation (SERI) under contract numbers 22.00173 and 24.00054; and by the UK Research and Innovation (UKRI) under the Department for Business, Energy and Industrial Strategy's Horizon Europe Guarantee Scheme.

The authors declare that the research was conducted in the absence of any commercial or other relationships that could be construed.

References

Anisimova, M., & Gascuel, O. (2006). Approximate likelihood ratio test for branches: A fast, accurate and powerful alternative. Systematic Biology, 55(4), 539–552.

Çakmak, Y. E., Soydabaş-Ayoub, H. K., & Uçkan, F. (2020). A preliminary phylogenetic analysis of ribbed pine borer (*Rhagium inquisitor*) based on mitochondrial COI sequences. Journal of Asia-Pacific Entomology, 23(3), 809–815.

Crowley, L. M., Poloni, R., Broad, G. R., Boyes, D., & Darwin Tree of Life Consortium (2024). The genome sequence of a longhorn beetle, *Stenurella melanura* (Linnaeus, 1758). Wellcome Open Research, 9, 414.

Gascuel, O. (1997). BIONJ: An improved version of the NJ algorithm based on a simple model of sequence data. Molecular Biology and Evolution, 14(7), 685–695.

Gouy, M., Tannier, E., Comte, N., & Parsons, D. P. (2021). SeaView version 5: A multiplatform software for multiple sequence alignment, molecular phylogenetic analyses, and tree reconciliation. Methods in Molecular Biology, 2231, 241–260.

Guindon, S., Dufayard, J.-F., Lefort, V., Anisimova, M., Hordijk, W., & Gascuel, O. (2010). New algorithms and methods to estimate maximum-likelihood phylogenies: Assessing the performance of PhyML 3.0. Systematic Biology, 59(3), 307–321.

Korlević, P., McAlister, E., Mayho, M., Makunin, A., Flicek, P., & Lawniczak, M. K. N. (2021). A minimally morphologically destructive approach for DNA retrieval and whole-genome shotgun sequencing of pinned historic dipteran vector species. Genome Biology and Evolution, 13(10), evab226.

Löbl, I., & Smetana, A. (Eds.). (2010). Catalogue of Palaearctic Coleoptera. Vol. 6: Chrysomeloidea. Stenstrup, Apollo Books.

Makunin, A., Korlević, P., Park, N., Goodwin, S., Waterhouse, R. M., von Wyschetzki, K., Jacob, C. G., Davies, R., Kwiatkowski, D., St. Laurent, B., Ayala, D., & Lawniczak, M. K. N. (2022). A targeted amplicon sequencing panel to simultaneously identify mosquito species and *Plasmodium* presence across the entire *Anopheles* genus. Molecular Ecology Resources, 22(1), 28–44.

Özdikmen, H., Mercan, N., & Cihan, N. (2012). A new species of the genus *Stenurella* Villiers, 1974 from Turkey (Coleoptera: Cerambycidae: Lepturinae). Munis Entomology and Zoology, 7(1), 18–21.

Rapuzzi, P., & Sama, G. (2009). Descriptions of new Cerambycidae from Greece, Turkey, Northern Syria and Southern Morocco (Coleoptera: Cerambycidae). Munis Entomology and Zoology, 4(1), 181–192.

Rapuzzi, P., Konvička, O., & Vít, D. (2011). The longhorn beetle *Stenurella sennii* (Coleoptera: Cerambycidae) in the Czech Republic and Croatia. Klapalekiana, 47, 237–238.

Sama, G. (2002). Atlas of the Cerambycidae of Europe and the Mediterranean Area. British Isles and Continental Europe from France (excl. Corsica) to Scandinavia and Urals. Vol. 1. Zlín, Nakladatelství Kabourek.

Sama, G., & Rapuzzi, P. (2011). Una nuova checklist dei Cerambycidae d'Italia (Insecta: Coleoptera: Cerambycidae). Quaderno di Studi e Notizie di Storia Naturale della Romagna, 32, 121–164.

Semaniuk, D. V., & Zamoroka, A. M. (2020). Preliminary phylogenetic analysis of Lepturini (Insecta: Coleoptera: Cerambycidae). In: Proceedings of the XVI International Scientific Conference for Students and PhD Students "Youth and Progress of Biology". Lviv. P. 121.

Sire, L., Gey, D., Debruyne, R., Noblecourt, T., Soldati, F., Barnouin, T., Parmain, G., Bouget, C., Lopez-Vaamonde, C., & Rougerie, R. (2019). The challenge of DNA barcoding saproxylic beetles in natural history collections: Exploring the potential of parallel multiplex sequencing with Illumina MiSeq. Frontiers in Ecology and Evolution, 7, 495.

Srivathsan, A., Feng, V., Suárez, D., Emerson, B., & Meier, R. (2024). ONTbarcoder 2.0: Rapid species discovery and identification with real-time barcoding facilitated by Oxford Nanopore R10.4. Cladistics, 40(2), 192–203.

Srivathsan, A., Lee, L., Katoh, K., Hartop, E., Kutty, S. N., Wong, J., Yeo, D., & Meier, R. (2021). ONTbarcoder and MinION barcodes aid biodiversity discovery and identification by everyone, for everyone. BMC Biology, 19(1), 217.

Touroult, J., Cima, V., Bouyon, H., Hanot, C., Horellou, A., & Brustel, H. (2019). Longicornes de France – Atlas préliminaire (Coleoptera: Cerambycidae & Vesperidae) [Longhorn beetles of France – preliminary atlas (Coleoptera: Cerambycidae & Vesperidae)]. Paris, Supplément au Bulletin d'ACOREP-France (in French).

Villiers, A. (1974). Une nouvelle nomenclature des Lepturines de France (Coleoptera: Cerambycidae) [A new nomenclature of Lepturins of France (Coleoptera: Cerambycidae)]. L'Entomologiste, 30, 207–217 (in French).

Vitali, F. (2018). Atlas of the insects of the Grand Duchy of Luxembourg: Coleoptera, Cerambycidae. Ferrantia, 79. Musée National d'Histoire Naturelle, Luxembourg.
Zamoroka A. M., Ruicănescu A., & Manci C.-O. (2024) East and West of the Carpathian Arc: Evidence of postglacial ecological and morphological divergence of Phytoecia tigrina metapopulations (Coleoptera, Cerambycidae). Biosystems Diversity, 32(1), 12–29.
Zamoroka, A. (2023). New additions to the fauna of the longhorn beetles in Ukraine with new records of rare, poorly known and invasive species. Baltic Journal of Coleopterology, 23(2), 159–188.
Zamoroka, A. (2025). When morphology meets molecules: Barcoding confirms an ancient separation of *Phytoecia tigrina* subspecies (Coleoptera: Cerambycidae). Zoodiversity, 59(5), 477–492.
Zamoroka, A. M. (2022). The longhorn beetles (Coleoptera: Cerambycidae) of Ukraine: Results of two centuries of research. Biosystems Diversity, 30(1), 46–74.
Zamoroka, A. M., Panin, R. Y., Kapelukh, Y. I., & Podobivskiy, S. S. (2012). The catalogue of the longhorn beetles (Coleoptera: Cerambycidae) of Western Podillya, Ukraine. Munis Entomology and Zoology, 7(2), 1145–1177.
Zamoroka, A. M., Semaniuk, D. V., Shparyk, V. Yu., & Mykytyn, T. V. (2019). Taxonomic position of *Anastrangalia reyi* and *A. sequensi* (Coleoptera: Cerambycidae) based on molecular and morphological data. Vestnik Zoologii, 53(3), 209–226.
Zamoroka, A. M., Trócoli, S., Shparyk, V. Y., & Semaniuk, D. V. (2022). Polyphyly of the genus *Stenurella* (Coleoptera: Cerambycidae): Consensus of morphological and molecular data. Biosystems Diversity, 30(2), 119–136.
Zamoroka, A., & Zinenko, O. (2025). Molecular cross-validation of intraspecific structure of *Rutpela maculata* (Insecta: Coleoptera: Cerambycidae). Journal of Vasyl Stefanyk Precarpathian National University. Biology, 12, 46–59.